Effect of Solvent Exchange on the Pore Structure and Dissolution Behavior of Cellulose

D. Ishii,* Y. Kanazawa, D. Tatsumi, T. Matsumoto

Division of Forest and Biomaterials Science, Graduate School of Agriculture, Kyoto University, Kyoto 606-8502, Japan

Received 12 May 2005; accepted 5 June 2006
DOI 10.1002/app.25424
Published online in Wiley InterScience (www.interscience.wiley.com).

ABSTRACT: Effect of solvent exchange, i.e., the sequential immersion in water, acetone, and DMAc on the pore structure of cellulose and its dissolution behavior in lithium chloride/*N*,*N*-dimethylacetamide (LiCl/DMAc) was investigated by using size exclusion liquid chromatography (SEC), dynamic light scattering (DLS), and small-angle X-ray scattering (SAXS). In the SEC experiment, poly(styrene)s, diethyl phthalate, and acetone were used as probe solutes and 2-butanone was used as an eluent. Capacity factor of these solutes in the solvent-exchanged cellulose were larger than those in the untreated one. This was remarkable when diethyl phthalate and acetone were used as solutes. Since the molecular radii of these solutes were estimated to be less than 1 nm, it was shown that the solvent exchange increases the amount of pores within cellulose with the radii of less than 1 nm. In the SAXS experiment, structural difference between the solvent exchanged and the untreated celluloses was observed when the celluloses were immersed in acetone. Values of specific inner surface and average chord length calculated from SAXS profile showed that the amount of small pores was increased in the solvent exchanged cellulose. Considering the results from SEC, DLS, and SAXS measurements, facilitated dissolution of the solvent exchanged cellulose in LiCl/DMAc was attributed to the increase in the pores with the radii of less than 1 nm. J Appl Polym Sci 103: 3976–3984, 2007

Key words: cellulose; swelling; pore structure; liquid chromatography; SAXS

INTRODUCTION

Cellulose is one of the most abundant natural polymers and thus used as a raw material in an extensive range of industries. Although the large portion of cellulose is used in solid state, the need for dissolving cellulose in appropriate solvents exists in some cases (e.g., the production of films and fibers). However, cellulose does not dissolve in conventional organic solvents for synthetic polymers, such as toluene, chloroform, tetrahydrofuran, and so on. Therefore, several kinds of solvents have been developed to dissolve cellulose.[1,2] Among them, lithium chrolide/*N*,*N*-dimethylacetamide (LiCl/DMAc) is regarded as the most effective one, because it can dissolve cellulose with high molecular weight more than 1.0×10^6.[3–5] However, prior to the dissolution of cellulose in LiCl/DMAc, pretreatment of cellulose by a method of solvent exchange is required.[3,4] In this method, cellulose is subsequently soaked in water, acetone, and DMAc at room temperature. Dissolution of cellulose is facilitated by such a simple method without the destruction of bulk morphology and crystalline structure.[6] Therefore, to clarify the reason why the dissolution of cellulose is facilitated by the solvent exchange, we have investigated the effect of the solvent exchange on the nanometer-scale solid structure and the molecular mobility of cellulose using solid-state NMR and small-angle X-ray scattering (SAXS).[6] As a result, it was shown that the solvent exchange affects nanometer-scale solid structure of cellulose. Although these spatial scales cover the microfibrillar morphology of cellulose,[1,2] it is supposed that the pore structure (size distribution and volume of pore) of cellulose within these spatial scales is also affected. From this point of view, the effect of the solvent exchange on the pore structure and the dissolution behavior of cellulose requires clarification.

Various methods have previously been proposed to investigate the pore structure of cellulose. Among them are included SAX/neutron scattering,[7–11] mercury intrusion,[12] gas sorption,[13] and ^{1}H broad-line NMR.[14] Size exclusion chromatography (SEC) also gives the information on the pore structure of cellulose and its derivatives.[15–25] This method has the advantage over other methods because it can investigate the pore structure of cellulose swollen in various kinds of liquids. However, previous studies focused only on the swelling of cellulose in water.[15–25] On the other hand, investigation of the swelling behavior of cellulose in other non-

Correspondence to: D. Tatsumi (daiske9@kais.kyoto-u.ac.jp).
**Present address:* Polymer Chemistry Laboratory, RIKEN (The Institute of Physical and Chemical Research), 2-1 Hirosawa, Wako, Saitama 351-0198, Japan.

Contract grant sponsor: Japan Society for the Promotion of Science; contract grant number: 16380118.

Journal of Applied Polymer Science, Vol. 103, 3976–3984 (2007)

aqueous media, which is required to clarify the effect of solvent exchange on the pore structure of cellulose, have not been performed yet. Therefore, we investigated the pore structure of cellulose in aqueous or nonaqueous media using SEC, DLS, and SAXS measurements. Based on the results of these experiments, differences in the pore structure in various media (water, acetone, and DMAc) and the relation between the pore structure and the dissolution behavior of cellulose in LiCl/DMAc will be discussed.

MATERIALS AND METHODS

Cellulose

Softwood dissolving pulp (DP, Nippon Paper Industries) and Whatman CF11 were used. These cellulose materials consist of the fibrillar particles having the size as follows: DP has the particle size of about 40 μm in diameter and a few millimeter in length[26]; CF11 has the particle size of about 20 μm in diameter and up to 350 nm in length.[27] These celluloses were immersed in water (once for 2 days) and then water was exchanged by acetone (twice for 1 day). For some of the acetone-treated celluloses, acetone was further exchanged by dimethylacetamide (DMAc) (twice for 1 day). These swollen celluloses (~ 1.5 g in dry weight) were stored in an Erlenmeyer flask, degassed using an aspirator and an ultrasonic water bath, and then packed in a stainless column (inner diameter of 6 mm and length of 250 mm) and supplied for the size exclusion chromatography (SEC) experiments. After the experiments were finished, the cellulose samples were vacuum-dried at 60°C and then weighed. Drying was continued until the sample weight reached the constant value. These oven-dry weight values were used for the correction of elution volume.

Size exclusion chromatography

Poly(ethylene glycol) (PEG) and poly(styrene) (PS) were chosen as solutes having various molecular sizes. Monodisperse PSs with different molecular weights (M_w = 380,000; 13,700; 4,000; 2,330; 820 (Aldrich Chemical, Milwaukee, MI); 200,000; 50,000; and 25,000 (Pressure Chemical, Pittsburgh, PA) were used. Polydispersity values (M_w/M_n) of all polystyrenes were less than 1.06. Molecular weight of PEG employed were 4000, 2000, 1500, 1000, 600, 400, 300, and 200 (Nacalai Tesque, Osaka, Japan). Diethyl phthalate (222) 1,3-dimethyl-2-imidazolidinone (DMI, 111), *N*,*N*-dimetyhlacetamide (DMAc, 87), and acetone (58) were also used as solutes (values in parentheses denote the molecular weights of the chemicals). Acetone, 2-butanone, toluene, and chloroform were used as eluents.

A conventional high-performance liquid chromatograph system (Shimadzu LC-10AT, equipped with 20 μL sample loop and RID-6A refractive index detector) was utilized for SEC experiments. A pumping speed and a column temperature were set to 1.0 mL/min and 40°C, respectively. To ensure the sufficient swelling of cellulose packed in the column, the eluent was flown overnight before the injection of the probe solutions. The concentration of the probe solutions was set to 1 mg/mL.

Size estimation of solute molecules

Two methods were employed for estimating the molecular size of the solutes used in the SEC experiments. For PSs that have relatively large molecular weights, dynamic light scattering (DLS) measurements were performed. In the DLS measurements, a scattered intensity of 632.8-nm He–Ne laser at the scattering angle of 30° was monitored using a multiangle laser light scattering photometer (SLS-5000HM, Otsuka Electoronics, Osaka, Japan) equipped with ALV5000/E Multiple Digital Tau Correlator (ALV-GmbH, Langen, Germany) at 40°C. The relation between the second-order time correlation function of the electric field of scattered light, $g^{(2)}(q, \tau)$, and τ was obtained (τ is the correlation time of scattering intensity fluctuation).

The function $g^{(2)}(q, \tau)$ is related to the first-order time correlation function in homodyne experiment, $g^{(1)}(q, \tau)$, by the equation below:

$$g^{(2)}(q,\tau) = 1 + \left|g^{(1)}(q,\tau)\right|^2. \quad (1)$$

The function $g^{(1)}(q, \tau)$ is related to $G(\Gamma)$, probability density function of the decay rate Γ, by

$$g^{(1)}(q,\tau) = \int_0^\infty G(\Gamma)\exp(-\Gamma\tau)d\Gamma. \quad (2)$$

Γ is related to the translational diffusion coefficient, D_T, by

$$\Gamma = D_T q^2. \quad (3)$$

Consequently, the hydrodynamic radius, R_H, is calculated from D_T by Einstein-Stokes equation:

$$R_H = \frac{k_B T}{6\pi\eta_s D_T} \quad (4)$$

where k_B and η_s denote Boltzmann constant and viscosity of the solvent, respectively.

In our experiment, regularized fitting with CONTIN method[28,29] was performed to obtain $G(\Gamma)$ from $g^{(2)}(q, \tau)$. The viscosity and the refractive index of the solvent needed for the estimation of R_H were estimated using a cone-plate-type rheometer (Rheosol-G2000, UBM, Kyoto, Japan) and an Abbe refractometer (NAR-1T, ATAGO, Tokyo, Japan) at 40°C, respectively.

The molecular sizes of low molecular weight solutes (acetone, diethyl phthalate, DMAc, and DMI) were not determined by DLS. Alternatively, ''solvent-excluded volume,''[30] V_{se}, a volume occupied by a given molecule in which the surrounding ''solvent'' molecules cannot penetrate, was calculated. In this method, using Chem3D Ultra (CambridgeSoft, Cambridge, MA), the molecular structures of solutes were optimized through MM2 procedure. Then, the V_{se} of solute molecules were calculated by setting the radius of ''solvent'' to 0.15 nm. Subsequently, the radius of the equivalent sphere, R_{se}, was calculated from V_{se} using the following equation:

$$R_{se} = ((3/4\pi)V_{se})^{1/3}. \quad (5)$$

In the following data treatment, R_{se} for low molecular solutes will be treated as equivalent to R_H for PSs, and the radii of all the solutes are referred to as ''molecular radius'' for simplicity. This treatment is justified by the previous finding that the hydrodynamic volume of the low molecular weight solute in the solution are roughly equal to the Van der Waals volume of the solute itself.[31]

Small-angle X-ray scattering

A 6-m point-focus SAXS (small-angle X-ray scattering) camera at the High-Intensity X-ray Laboratory of Kyoto University was utilized.[32] The sample-to-detector distance was set to 1.6 m, covering the real-space length scales between 3 and 40 nm. Wet cellulose samples were packed in a homemade stainless cell[33] with Kapton windows. A scattered intensity of Cu Kα irradiation ($\lambda = 0.1542$ nm, 40 kV, and 50 mA) was acquired using two-dimensional position-sensitive proportional counter for more than 10,000 s. Then, the two-dimensional profile was corrected for transmittance, incident beam intensity (calibrated using high-density polyethylene as secondary standard), and the scattering intensity from swelling media (water, acetone, or DMAc). Finally, the corrected profile was circularly averaged and one-dimensional profile was obtained.

RESULTS AND DISCUSSION

Appropriate choice for eluent and solute

In most of the previous SEC experiments, water was used as an eluent and PEG or other various water-soluble substances (e.g., D_2O, NaCl, and various kinds of mono- or oligosaccharides) as solutes.[15–25] However, the use of water as eluent is not suitable for our purpose, because the immersion of the DMAc-treated cellulose in water spoils the effect of the solvent exchange. For example, the solubility of the DMAc-treated cellulose in LiCl/DMAc is lowered by the immersion in water. It is supposed that the change in the pore structure of cellulose that may be caused by the solvent exchange is cancelled out by the immersion in water. Therefore, we explored the suitable choices for the eluent and the solute that enables us to detect the difference in the pore structure between the untreated and the solvent-exchanged celluloses.

What is needed for solute material is (a) availability of materials covering the broad ranges of molecular weight and (b) monodispersity of molecular weight in each materials. The former prerequisite enables us the investigation of pores with broad ranges of size. The latter one is needed for the correctness of the evaluation of size of pore accessed by the solute. Among the commercial polymers, PEG and PS were chosen as candidate to satisfy the above-mentioned prerequisites. Furthermore, what is needed for eluents is (a) working as a good solvent for the solute, (b) an ability to preserve the effect of solvent exchange on cellulose, and (c) no sorption of the solute occurs onto cellulose swollen in the eluent. Considering these prerequisites, acetone, 2-butanone, toluene, and chloroform were chosen as candidates.

Elusion behavior of the solutes so much varied dependent on the choice for the eluent. When PS and 2-butanone were used as the solute and the eluent, respectively, sharp chromatogram was obtained [Fig. 1(a)]. No such chromatograms were obtained using the other combinations of the eluents and the solutes. For example, when PEG and acetone were used, a quite unresolved chromatogram was obtained [Fig. 1(b)]. This seemed due to the sorption of PEG on cellulose. Consequently, 2-butanone and PS were chosen as the eluent and the solute. (In Appendix, whether the solutes and solvents thermodynamically interact with cellulose is examined by using the concept of Hansen solubility parameter.)

The elusion behavior of the solute from a chromatography column is generally determined by the hydrody-

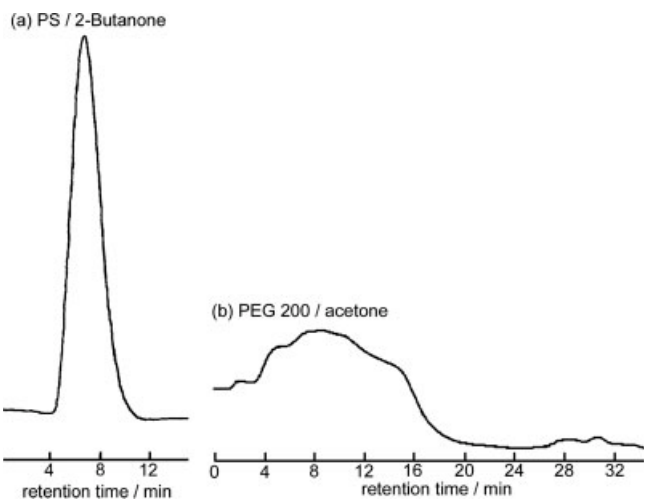

Figure 1 Chromatogram of (a) poly(styrene) in 2-butanone and (b) poly(ethylene glycol) in acetone.

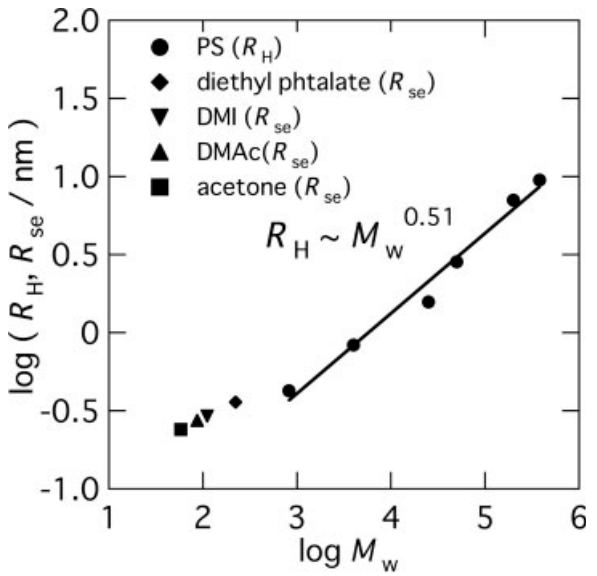

Figure 2 Relation between the molecular radius and the molecular weight, M_w, of solutes. As for poly(styrene)s, the hydrodynamic radius, R_H, is plotted. On the other hand, for low molecular weight solutes (diethyl phthalate, DMI, DMAc, and acetone), the radius of the equivalent sphere of ''solvent-excluded'' volume, R_{se}, is plotted.

namic volume of solute molecules.[34] To evaluate the radius of hydrodynamic equivalent sphere of solute molecules, R_H, DLS measurements were performed. Figure 2 shows the relation between R_H for PSs or R_{se} for low molecular solutes and M_w for solutes. Relation between both values in PSs is described by a power law with a power of 0.51. This value is lower than the usual one (about 0.60) previously found for this system[35] but corresponds to that found for PEG in water.[25] However, the exponent seems to coincide with the usual one when only high molecular weight fractions (above 25,000) are taken into account. Therefore, it is supposed that the reason for the relatively low exponent may be the inclusion of low molecular weight fractions, where the deviation from Gaussian statistics of chain dimension is assumed. The deviation is also found for nonpolystyrene materials, i.e., diethyl phthalate and acetone. Nevertheless, it can be said that the differences in molecular weight of the solutes correspond to the differences in molecular diameters. This ensures that the solutes with different molecular weights can penetrate the pores with different diameters.

Elusion patterns of cellulose by SEC

The above set of the solutes and the eluent were introduced to the celluloses in the chromatography column, and the size exclusion of the solute molecules was attempted. Figure 3 shows the chromatograms of PSs with different molecular weights. The elusion time of each PS gradually increased with decreasing molecular weight. This demonstrates that the elusion behavior of PS from cellulose is governed only by the molecular size of PS. This ensures the appropriateness of PS as the probes for the investigation of the pore structure of cellulose. The elusion volume of each solute, V_e, was calculated using the following equation:

$$V_e = tv_0/w \tag{6}$$

where t_e, v, and w denote the elusion time at the peak of chromatogram, a pumping speed, and the weight of cellulose packed in the column, respectively.

In Figure 4, logarithm of molecular weight, M_w, is plotted versus the elusion volume, V_e (in milliliter per gram), of PSs and other low-molecular weight solutes (diethyl phthalate, DMI, DMAc, and acetone). The V_es of DMI and DMAc were significantly larger than the other solutes. This shows that the strong intermolecular interaction works between DMI or DMAc and cellulose. As for the solutes other than DMI and DMAc, V_e gradually increased with decreasing molecular weights of solutes in the respective experiments. However, V_es for each solute largely varied among the respective experiments. It was supposed that such large variation comes from the difference in the amount of cellulose packed in the column. Therefore, V_e was transformed into capacity factor to correct the variation.

Capacity factor, k', is defined as a ratio of quantity of solute in between the mobile phase (void) and stationary phase (pore).[24,36] Assuming that the ratio of concentration between the mobile phase and stationary phase is independent on the molecular size of solute, k' is

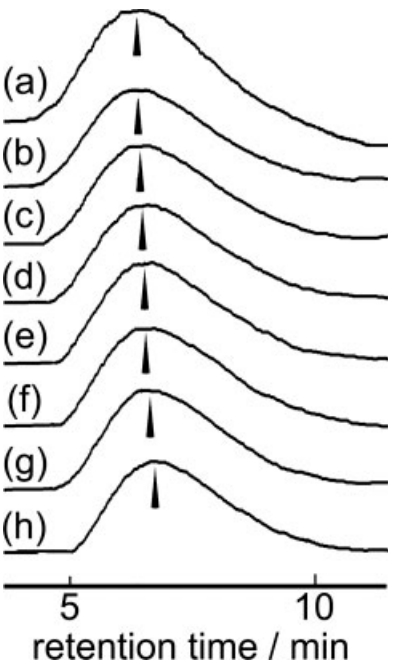

Figure 3 Chromatograms of poly(styrene)s with different molecular weights: (a) 380,000; (b) 200,000; (c) 50,000; (d) 25,000; (e) 13,700; (f) 4000; (g) 2330; and (h) 820. Triangles show the points to obtain the values of elution time.

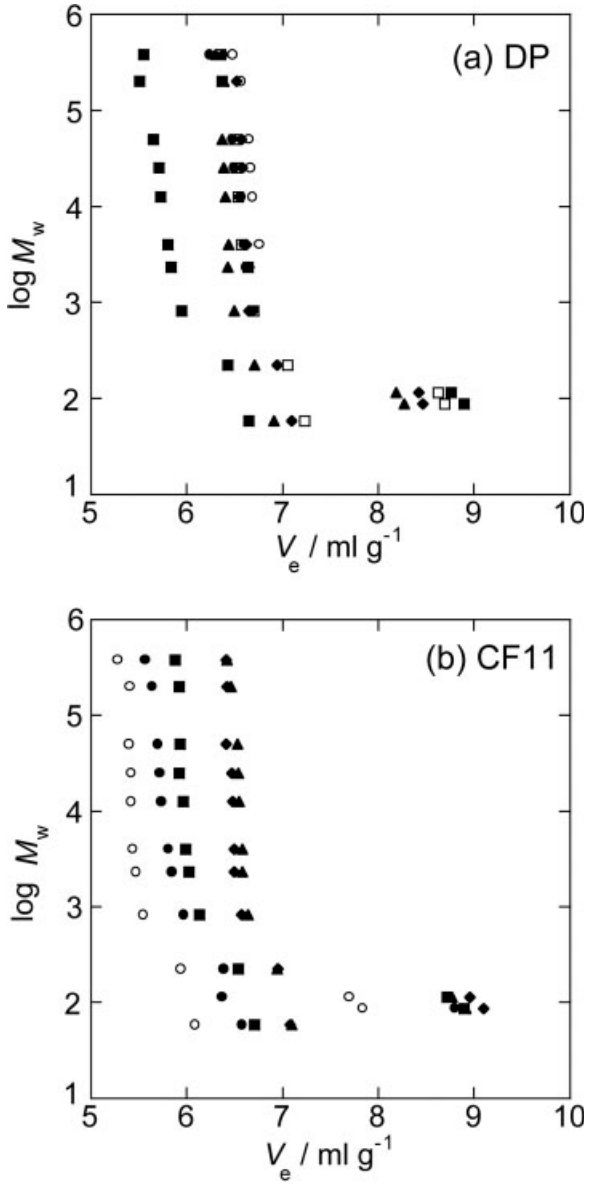

Figure 4 Elusion volume of poly(styrene)s and other low-molecular weight solutes (diethyl phthalate, DMI, DMAc, and acetone) in (a) the untreated and (b) the DMAc-treated celluloses. Open and filled symbols designate the values obtained for untreated and DMAc-treated cellulose, respectively. For both celluloses, the experiments were repeated and the values obtained from the respective experiments are distinguished by the shapes of the symbols.

equal to the ratio between the volumes of the mobile phase and stationary phase. In such a case, k' can be used as an indicator of the proportion of pores contributing to the gel permeation effect. In our experiments, the condition is satisfied, because the chromatograms of each PS showed no difference in shapes irrespective of its molecular weight.

Exact values of k' is thus given in the equation below:

$$k' = (V_e - V_m)/V_m \quad (7)$$

where V_e and V_m denote the elusion volume of a given solute and the one at the exclusion limit, respectively. In our experiment, V_e of PS with the M_w of 380,000 was used as V_m.

The cumulative values of the capacity factor, k', of the solutes is plotted versus the molecular weight, M_w, of the solutes (except DMAc and DMI) as shown in Figure 5. It is found that k' is especially large for the solutes with relatively low molecular weight. This shows that the pores having relatively small diameters dominantly exist. It is also found that, both for DP and CF11, the DMAc-treated celluloses have more amount of pores with small diameters than the acetone-treated ones. This shows that the DMAc treatment increases the amount of pores having small diameters. Figure 6 shows the relation between k' and molecular radius, R, of the solutes. This indicates that the DMAc treatment increases the amount of pores in which the solutes with the R of less than 1 nm can penetrate. As shown in

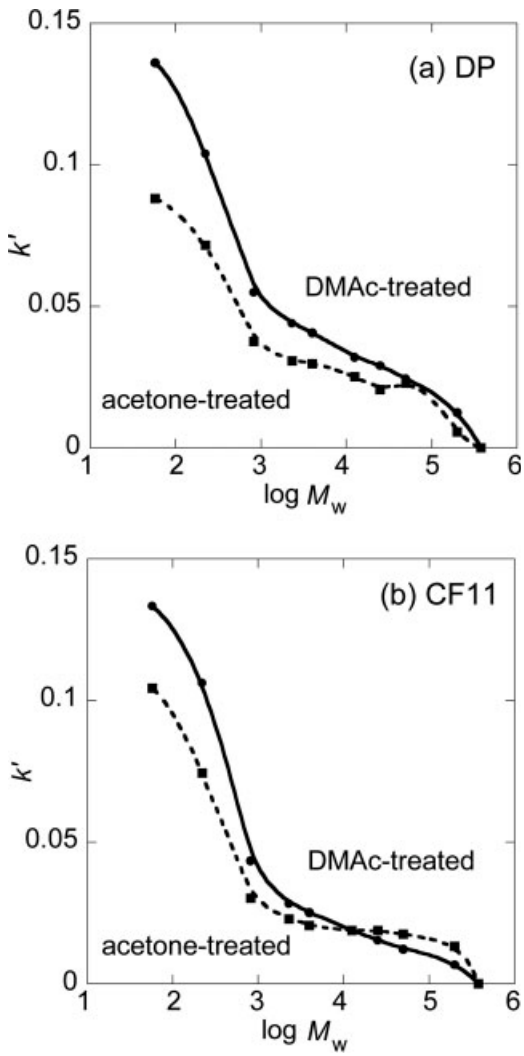

Figure 5 Relation between the capacity factor, k', and the molecular weight, M_w, of solutes eluted from (a) the untreated and (b) the DMAc-treated celluloses.

Figure 2, these length scales correspond to the molecular size of the solvent for cellulose, i.e., DMAc and DMI. Therefore, it is concluded that the facilitated dissolution of the DMAc-treated cellulose in LiCl/DMAc is attributed to the increase in the small-size pore corresponding to the solvent molecules within cellulose.

SAXS measurements

The SAXS measurements were performed to obtain information on the pore structure of cellulose complementary to the SEC data. Figure 7 shows SAXS profiles of the cellulose samples (the untreated and the DMAc-treated DP) in water, acetone, and DMAc. The scattered intensity $I(q)$ is plotted versus the magnitude of scattering vector, $q = (4\pi/\lambda) \sin(\theta/2)$ (θ, the scattering angle). Differences in the structure between the untreated and the DMAc-treated celluloses were found only when acetone was used as a medium. This shows that acetone and its analogues are appropriate for the mobile phase in SEC for the investigation of the structural difference induced by the solvent exchange. Since 2-butanone has similar chemical structure and properties to acetone, appropriateness of the choice of 2-butanone for the eluent in the SEC was confirmed. On the other hand, when water was used as a medium, no structural difference between the untreated and the DMAc-treated cellulose was found. This can be related to the fact that the sorption of the DMAc-treated cellulose in water spoils the effect of the solvent exchange.

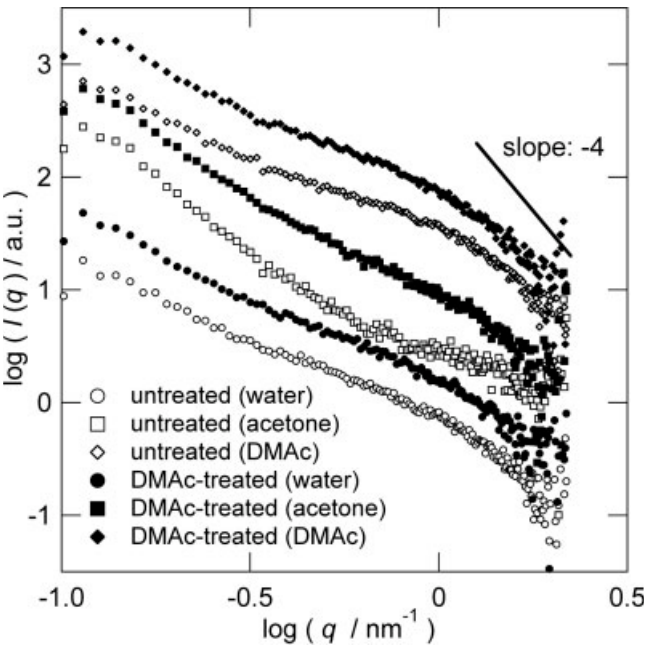

Figure 7 SAXS profiles of cellulose solid (dissolving pulp) in water, acetone, or DMAc.

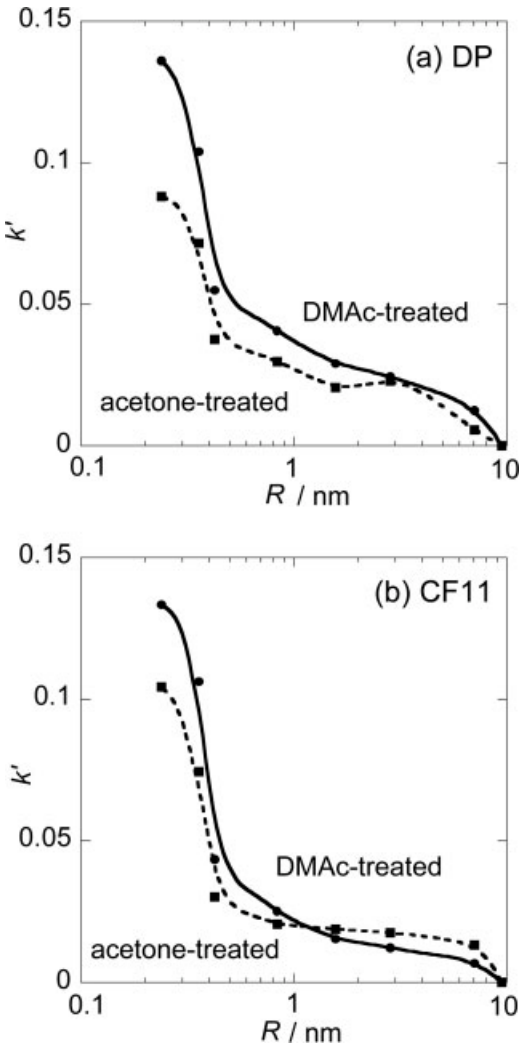

Figure 6 Relation between the capacity factor, k', and the hydrodynamic radius, R_H, of solutes eluted from (a) the untreated and (b) the DMAc-treated celluloses.

Various kinds of structural parameters were obtained from SAXS profiles. First, we evaluated the size of the scattering bodies using Guinier approximation,[37] i.e.,

$$I(q) = G \exp\left(-\frac{R_g^2}{3} q^2\right), \quad qR_g < 1 \tag{8}$$

where R_g denotes the radius of gyration of scattering bodies.* Figure 8 shows the Guinier plot, i.e., the plot of ln [$I(q)$] vs. q^2 of swollen cellulose (untreated DP in water). Plots at low-q region ($q < 0.04$ nm^{-1}) were approximated using eq. (8), and R_g was calculated.

*Two assumptions for the structural origin that gives R_g can be made: One is the cellulose microfibril and the other is the large pore. We have formerly shown that the structural heterogeneity of cellulose in the dried state as observed by SAXS is evaluated by fractal dimension.[6] Because the fractal nature originates in the aggregation of cellulose microfibril, it is considered that the value of R_g reflects the size of cellulose microfibril as an elemental structural unit of cellulose.

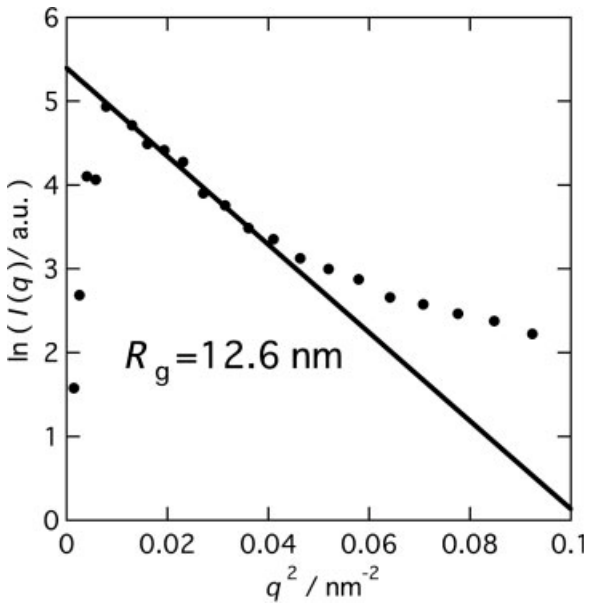

Figure 8 A typical Guinier plot of swollen cellulose (untreated dissolving pulp in acetone).

Next, we investigated the surface structure of cellulose using Porod approximation.[38] In Porod approximation, scattered intensity is expressed as follows:

$$\lim_{q\to\infty} I(q) = \frac{K_p}{q^4}. \tag{9}$$

Figure 9 shows the Porod plot, i.e., the plot of $q^4I(q)$ vs. q^4 of the swollen cellulose. At large-q region ($q > 1.5$ nm^{-1}), the plots converged to a constant value, although there was somewhat a large variation. This shows that the boundary of the electron density at the cellulose surface in the mentioned spatial scales is defined. The Porod constant, K_p, is defined by[38]

$$K_p \equiv 2\pi S(\rho_c - \rho_s)^2 = \frac{1}{\pi}\frac{S}{V}\frac{Q}{\phi(1-\phi)}. \tag{10}$$

where S, V, and ϕ in eq. (10) denote surface area, volume, and volume fraction of pore, respectively. The ρ_c

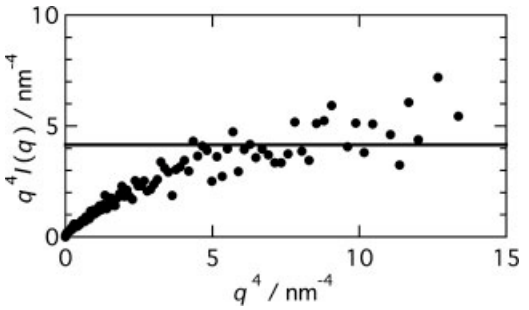

Figure 9 A typical Porod plot of wet cellulose (untreated dissolving pulp in acetone). A straight line represents K_p, the limiting value of the plot.

and ρ_s denote the electron density of cellulose and medium. The Q is referred to as invariant and defined by the equation below[38]:

$$Q \equiv 2\pi^2 V(\rho_c - \rho_s)^2\phi(1-\phi) = \int_0^\infty q^2 I(q)dq. \tag{11}$$

Equation (11) shows that the integration of $q^2I(q)$ over q gives the value of Q. To perform the integration, Guinier and Porod approximations were applied in the small-q and large-q regions, respectively. The actual calculation of Q was thus performed using the following equation:[10]

$$Q = \sum_{q=0}^{q_{\min}} q^2 I_{\text{Guinier}}(q)\Delta q + \sum_{q=q_{\min}}^{q_{\max}} q^2 I_{\text{obsd}}(q)\Delta q + \sum_{q=q_{\max}}^{\infty} q^2 I_{\text{Porod}}(q)\Delta q \tag{12}$$

where $I_{\text{Guinier}}(q)$, $I_{\text{Porod}}(q)$, and $I_{\text{obsd}}(q)$ denote the intensities defined by the eqs. (8) and (9), and experimentally obtained. The values $q_{\min}$ and $q_{\max}$ ($q_{\min} < q_{\max}$) denote the values of q at the lower and the upper cutoffs of the q-regions where $I_{\text{obsd}}(q)$ was used for the calculation of Q. Figure 10 shows the Kratky plot, i.e., the plot of $q^2I(q)$ vs. q, for the untreated and the DMAc-treated celluloses. Curves in the small-q and large-q regions represent the Guinier and the Porod equations, respectively. These curves show that the plots converge to zero both in the small- and large-q limits and that the integration of $q^2I(q)$ over q is thus possible. The value of Q calculated from the plot was assigned to eq. (10), for evaluating the heterogeneity of cellulose.

In the following discussion, we employ two measures to evaluate the heterogeneity of cellulose. One measure is the specific inner surface, $O_s = S/V$, of cellulose. To calculate O_s, the capacity factor of acetone was assigned to the volume fraction of pore, ϕ.

The other measure is the average chord length, l_c.* It reflects the average sizes of pore and solid in porous materials. The value of l_c is calculated by

$$l_c = 4\phi(1-\phi)\frac{V}{S} = \frac{4}{\pi}\frac{Q}{K_p}. \tag{13}$$

The length l_c is related to the average sizes of pore and solid, l_p and l_s, by*

$$l_c = (1-\phi)l_p = \phi l_s. \tag{14}$$

The calculated values of O_s, l_c, l_p, l_s, and R_g of celluloses in acetone are shown in Table I. It is found that O_s of the DMAc-treated cellulose is larger than that of the

*See footnote on page 3981.

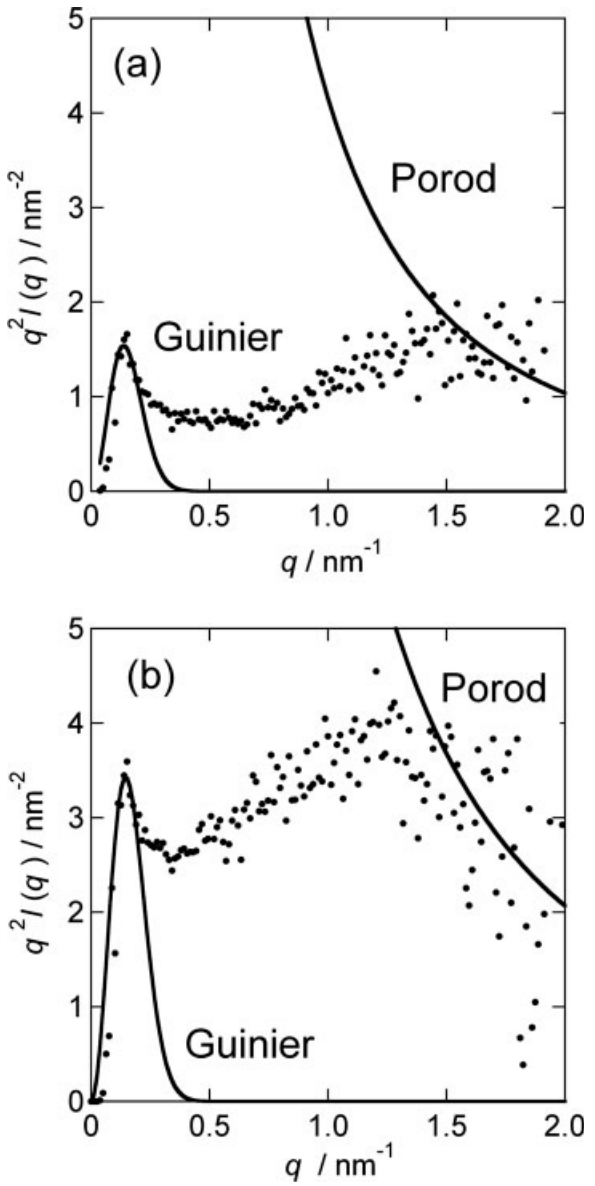

Figure 10 Kratky plots of cellulose (dissolving pulp) in acetone: (a) untreated and (b) DMAc-treated ones. Curves in the small- and large-q regions represent the Guinier and Porod approximations given from eqs. (8) and (9), respectively.

untreated one. This shows that the surface area of cellulose is increased by the DMAc treatment. The length l_p is almost unaffected by the DMAc treatment, while l_s is lowered. This shows that the DMAc treatment increases the amount of small pores in cellulose and thus the surface roughness of cellulose. The increase in the amount of small pores was confirmed by the SEC measurement that showed an increase in the amount of pores with the radii of less than 1 nm. The increase in the surface roughness of cellulose has been already shown by the increase in the fractal dimension, although it was investigated in the dried state.[6] Considering these results, it is concluded that the increase in the amount of small pores induced by the DMAc treatment leads to the enlargement of the surface area and consequently facilitates the access of solvent molecules to the cellulose solid, resulting in the facilitated dissolution in LiCl/DMAc.

TABLE I
Characteristic Values of the Structure of Cellulose Solid (Dissolving Pulp) in Acetone

	ϕ[a]	O_s (nm^{-1})	l_c (nm)	l_p (nm)	l_s (nm)	R_g (nm)
Untreated	0.088	0.469	0.684	0.514	5.33	12.6
DMAc-treated	0.136	0.514	0.914	0.594	3.78	11.8

[a] Capacity factor of acetone, as determined by the SEC measurement, was assigned to ϕ.

APPENDIX

We judged whether the solutes chosen in this work (see the section ''Appropriate choices for eluent and solute'') interact with cellulose by using the concept of Hansen solubility parameter.[39] In this concept, Hildebrand solubility parameter (δ) of each compound is decomposed into three terms, i.e., dispersion (δ_D), polarity (δ_P), and hydrogen bonding (δ_H) ones ($\delta^2 = \delta_D^2 + \delta_P^2 + \delta_H^2$). The value of δ_D, δ_P, and δ_H for various chemicals is listed in the aforementioned literature.[39] Each compound is characterized by δ_D, δ_P, and δ_H and located in the $\delta_D - \delta_P - \delta_H$ three-dimensional coordinate system. In this space, polymers occupy the spherical region in which compounds are regarded as interacting with the polymer. The sphere is called as ''solubility sphere'' and defined by the δ_D, δ_P, and δ_H of a mentioned polymer (being a center of the sphere) and interaction radii R. Larger value of R means that the polymer can interact with more compounds. The solubility parameters (δ_D, δ_P, and δ_H) of the solutes used in our work are listed in Table AI. Value of R is also shown for the polymers used (cellulose and PS). It is readily found that δ_D does not vary so much while δ_P and δ_H considerably varies among the solutes. Therefore, each solute was compared by only δ_P and δ_H. Figure A1 shows the $\delta_P - \delta_H$

TABLE AI
Hansen Solubility Parameters of Polymers, Solutes, and Solvents Used in This Work

	δ_D/ (MPa)$^{1/2}$	δ_P/ (MPa)$^{1/2}$	δ_H/ (MPa)$^{1/2}$	R
Cellulose	24.3	19.9	22.5	17.4
Poly(styrene)	18.5	4.5	2.9	5.3
Acetone	15.5	10.4	7.0	
2-Butanone	16.0	9.0	5.1	
Chloroform	17.8	3.1	5.7	
Diethyl phthalate	17.6	9.6	4.5	
DMAc	16.8	11.5	10.2	
Toluene	18.0	1.4	2.0	

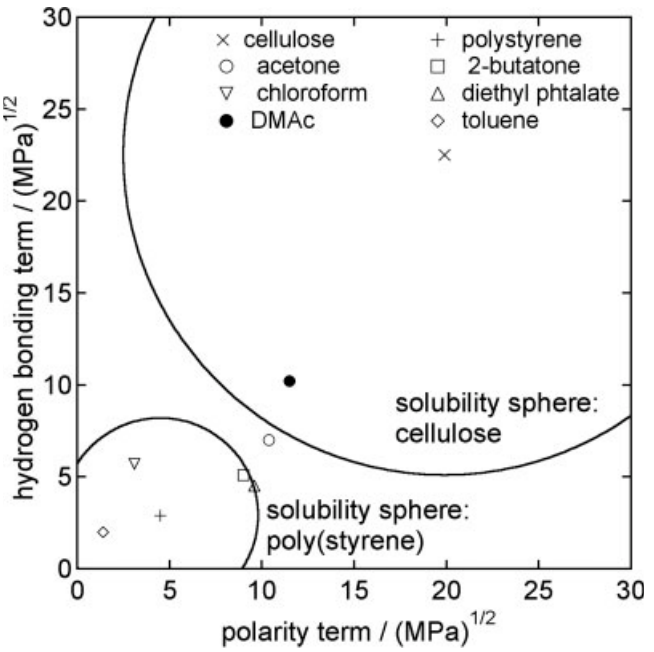

Figure A1. Plot of two interaction parameters, δ_P and δ_H, of the polymers, solutes, and solvents used in this work.

plot of the solutes and eluents used. The solubility spheres of cellulose and PS are also shown. In this plot, only DMAc is located within the solubility sphere of cellulose. Therefore, it is regarded that DMAc interacts with cellulose. This is consistent with SEC result that the elution time of DMAc was longer than other solutes (Fig. 4). On the other hand, other solutes lie outside the solubility sphere of cellulose but within or near that of PS. This shows that the effect of the thermodynamic interaction between cellulose and the solutes on their elution behavior can be considered negligibly small. Therefore, it is regarded that the solutes except DMAc is not adsorbed onto cellulose.

References

1. Johnson, D. C. In Cellulose Chemistry and Its Applications; Nevell, T. P., Zeronian, S. H., Eds.; Ellis Horwood: Chichester, UK, 1985; p 185.
2. Klemm, D.; Philipp, B.; Heinze, T.; Heinze U.; Wagenknecht, W. In Comprehensive Cellulose Chemistry, Vol. 1; Wiley-VCH: Weinheim, Germany, 2001; p 150.
3. Turbak, A. Tappi J 1984, 67, 94.
4. McCormick, C. L.; Callais, P. A.; Hutchinson, B. H., Jr. Macromolecules 1985, 18, 2394.
5. Matsumoto, T.; Tatsumi, D.; Tamai, N.; Takaki, T. Cellulose 2002, 8, 275.
6. Ishii, D.; Tatsumi, D.; Matsumoto, T. Biomacromolecules 2003, 4, 1238.
7. Crawshaw, J.; Cameron, R. E. Polymer 2000, 41, 4691.
8. Crawshaw, J.; Vickers, M. E.; Briggs, N. P.; Heenan, R. K.; Cameron, R. E. Polymer 2000, 41, 1873.
9. Vickers, M. E.; Briggs, N. P.; Ibbett, R. N.; Payne, J. J.; Smith, S. B. Polymer 2001, 42, 8241.
10. Astley, O. M.; Donald, A. M. Biomacromolecules 2001, 2, 672.
11. Astley, O. M.; Chanliaud, E.; Donald, A. M.; Gidley, M. J Int J Biol Macromol 2001, 29, 193.
12. Stone, J. E.; Scallan, A. M.; Aberson, G. M. A. Tappi J 1966, 49, T265.
13. Stone, J. E.; Scallan, A. M. Pulp Pap 1965, 66, T407.
14. Li, T.-Q.; Henriksson, U.; Odberg, L. Nord Pulp Pap Res J 1993, 3, 326.
15. Aggebrandt, L. G.; Samuelson, O. J Appl Polym Sci 1964, 8, 2801.
16. Stone, J. E.; Scallan, A. M. Tappi J 1967, 50, 496.
17. Stone, J. E.; Scallan, A. M. Cellul Chem Technol 1968, 2, 343.
18. Nelson, R.; Oliver, D. W. J Polym Sci C 1971, 36, 305.
19. Kuga, S. J Chromatogr 1981, 26, 449.
20. Rowland, S. P.; Wade, C. P.; Bertoniere, N. R. J Appl Polym Sci 1984, 29, 3349.
21. Bertoniere, N. R.; King, W. D. Text Res J 1989, 59, 114.
22. Bredereck, K.; Blüher, A. Melliand Textilberichte 1992, 73, 652.
23. Broek, A. P.; Teunis, H. A.; Bargeman, D.; Sprengers, E. D.; Strathmann, H.; Smoulders, C. A. J Membr Sci 1995, 99, 217.
24. Kasahara, K.; Sasaki, H.; Donkai, N.; Ito, H.; Takagishi, T. Sen'I Gakkaishi 2002, 58, 332.
25. Keim, C.; Li, C.; Ladisch, C. M.; Ladisch, M. Biotechnol Prog 2002, 18, 317.
26. http://www.npchem.co.jp/product/dp/dp_02.html (In Japanese).
27. Qiu, J.; Zhang, F.; Endo, T.; Hirotsu, T. J Mater Sci 2005, 40, 3607.
28. Provencher, S. W. Comput Phys Commun 1982, 27, 213.
29. Provencher, S. W. Comput Phys Commun 1982, 27, 219.
30. Connolly, M. L. J Am Chem Soc 1985, 107, 1118.
31. Zhang, Y.; Sluch, M. I.; Somoza, M. M.; Berg, M. A. J Chem Phys 2001, 115, 4212.
32. Hayashi, H.; Hamada, F.; Suehiro, S.; Ogawa, T.; Miyaji, H. J Appl Crystallogr 1988, 21, 330.
33. Koyama, H.; Yoshizaki, T.; Einaga, Y.; Hayashi, H.; Yamakawa, H. Macromolecules 1991, 24, 932.
34. Grubisic, Z.; Rempp, P.; Benoit, H. J Polym Sci Polym Lett 1967, 5, 753.
35. Kurata, M.; Tsunashima Y. In Polymer Handbook, 4th ed.; Brundrup, J., Immergut, E. H., Grulke, E. A., Eds.; Wiley: New York, 1999; Chapter VII, p 69.
36. Glöckner, G. Polymer Characterization by Liquid Chromatography (J Chromatogr Library 34, 568); Elsevier: Amsterdam, 1986; p 33.
37. Guinier, A. Ann Phys 1939, 12, 161.
38. Porod, G. In Small Angle X-ray Scattering; Glatter, O., Kratky, O., Eds.; Academic Press: London, 1982; Chapter 2.
39. Hansen, C. M. Hansen Solubility Parameters: A User's Guidebook; CRC Press: Boca Raton, 2000.